The effect of flows on transverse oscillations of coronal loops.

M. S. Ruderman (m.s.ruderman@sheffield.ac.uk)
Solar Physics and Space Plasma Research Centre (SP^{2}RC), Department of Applied Mathematics, University of Sheffield, Hicks Building, Hounsfield Road, Sheffield, S3 7RH, UK

September 1, 2010

Abstract. In this paper we study kink oscillations of coronal loops in the presence of flows. Using the thin tube approximation we derive the general governing equation for kink oscillations of a loop with the density varying along the loop in the presence of flows. This equation remains valid even when the density and flow are time-dependent. The derived equation is then used to study the effect of flows on eigenfrequencies of kink oscillations of coronal loops. The implication of the obtained results on coronal seismology is discussed.

1. Introduction

Since transverse oscillations of coronal loops were first observed by Transition Region and Coronal Explorer (TRACE) and subsequently interpreted as fast kink oscillations of magnetic flux tubes, the theory of kink oscillations of magnetic flux tubes remains among the hot topics in solar physics. In early theoretical studies only straight homogeneous static tubes with circular cross-sections were considered. In recent years the theory was extended in different directions. For a recent review of the theory of coronal loop kink oscillations see, *e.g.*, Ruderman and Erdélyi (2009).

Observations by Solar and Heliospheric Observatory (SoHO) (see Brekke, Kjeldseth-Moe, and Harrison, 1997; Winebarger *et al.*, 2002), TRACE (see Winebarger, DeLuca, and Golub, 2001) and more recently Hinode (see *e.g.* Chae *et al.*, 2008; Ofman and Wang, 2008; Terradas *et al.*, 2008) show that flows are ubiquitous in active region loops. Hence, it is important to study how flows in coronal loops modify the properties of kink oscillations.

Gruszecki, Murawski, and Ofman (2008) have studied numerically kink oscillations of coronal loops in the presence of field-aligned flow using the slab model. Recently Terradas, Goossens, and Ballai (2010) studied the effect of flows on the period and damping rate of propagating kink oscillations in a tube homogeneous in the longitudinal direction. In this paper we aim to study the effect of flows on standing kink oscillations of a loop with the density varying along the loop.

The paper is organized as follows. In the next section we formulate the problem and write the linearized system of governing equations and boundary conditions. In Section 3 we use the thin tube approximation to derive the general governing equation for kink oscillations in a loop with time-dependent density and flow. In Section 4 we use this equation to study kink oscillations of a magnetic tube with homogeneous stationary density and flow. In Section 5 we describe the general properties of the eigenvalues problem for kink oscillations of a tube with stationary density and flow. In Section 6 we consider a particular equilibrium with the flow confined in the tube, and study the effect of a steady flow on the frequencies of the fundamental harmonic and first overtone of kink oscillations for this particular equilibrium. Section 7 contains the summary of the obtained results and our conclusions.

2. Problem formulation

We consider kink oscillations of a thin straight magnetic flux tube with circular cross-section. The tube is not expanding, so that the cross-section radius remains constant and equal to a. The plasma density in the tube and in the surrounding plasma can vary along the tube and with time. Hence, in cylindrical coordinates r, φ, z with the z-axis coinciding with the tube axis the unperturbed plasma density is $\rho(t,z)$. In addition, there is a plasma flow along the tube with the velocity $U(t,z)$. The plasma density and velocity are related by the mass conservation equation,

$$\frac{\partial \rho}{\partial t}+\frac{\partial (\rho U)}{\partial z}=0. \tag{1}$$

We do not consider physical processes that cause the density variation, so that we do not use the momentum and energy equations for the unperturbed quantities. The unperturbed magnetic field is everywhere in the z-direction and has constant magnitude B.

To describe the plasma motion we use the ideal linearized MHD equations for a cold plasma,

$$\frac{\partial \mathbf{v}}{\partial t}+(\mathbf{U}\cdot\nabla)\mathbf{v}+(\mathbf{v}\cdot\nabla)\mathbf{U}=\frac{1}{\mu_0\rho}[(\nabla\times\mathbf{b})\times\mathbf{B}+(\nabla\times\mathbf{B})\times\mathbf{b}], \tag{2a}$$

$$\frac{\partial \mathbf{b}}{\partial t}=\nabla\times(\mathbf{v}\times\mathbf{B}+\mathbf{V}\times\mathbf{b}), \tag{2b}$$

$$\nabla\cdot\mathbf{b}=0. \tag{2c}$$

Here $\mathbf{v}$ and $\mathbf{b}$ are the perturbations of the velocity and magnetic field, and μ_0 the magnetic permeability of free space. Taking into account

that $\mathbf{U} = U\mathbf{e}_z$ and $\mathbf{B} = B\mathbf{e}_z$, where $\mathbf{e}_z$ is the unit vector in the z-direction, we obtain from Equation (2a) that $v_z = 0$.

The system of equations (2) has to be supplemented with the boundary conditions. At the tube boundary the dynamic and kinematic boundary conditions have to be satisfied. The linearized dynamic boundary condition is that the perturbation of the magnetic pressure, $P = Bb_z/\mu_0$, has to be continuous,

$$[\![P]\!] = 0, \quad \text{at} \;\; r = a, \tag{3}$$

where $[\![f]\!]$ indicates the jump of a function f across the boundary. Let the equation of the perturbed tube boundary be $r = a+\eta(t, \varphi, z)$. Then the linearized kinematic boundary condition is

$$v_r = \frac{\partial \eta}{\partial t} + U\frac{\partial \eta}{\partial z} \quad \text{at} \;\; r = a. \tag{4}$$

Since the tube surface is a tangential discontinuity, the normal component of the magnetic field at the tube surface is zero. This condition is written as

$$b_r - B\frac{\partial \eta}{\partial z} = 0 \quad \text{at} \;\; r = a. \tag{5}$$

The boundary conditions (4) and (5) are not independent. It is straightforward to show using Equation (2b) that the second boundary condition follows from the first one.

Finally, we use the fact that the magnetic field lines are frozen in the dense photospheric plasma to obtain the boundary conditions at $z = \pm L/2$. When there is no equilibrium flow these conditions are simply $\mathbf{v} = 0$. However in the presence of equilibrium flow they become more complicated. The best way to obtain these boundary conditions is to make use of one of the two universal boundary conditions of electrodynamics, namely, the condition that the tangential component of the electrical field, $\mathbf{E}_\tau$, is continuous at any surface. Recall that, in ideal MHD, the electrical field $\mathbf{E}$ is given by

$$\mathbf{E} = -(\mathbf{U} + \mathbf{v}) \times (\mathbf{B} + \mathbf{b}).$$

Since in the regions $|z| > L/2$ the magnetic field lines are straight and the plasma can flow only along the magnetic field lines, $\mathbf{E} = 0$ in these regions, which implies that $\mathbf{E}_\tau = 0$ at $z = \pm L/2$. Then, linearizing these boundary conditions and taking into account that both $\mathbf{U}$ and $\mathbf{B}$ are parallel to the z-direction, we immediately obtain that

$$B\mathbf{v} - U\mathbf{b}_\perp = 0 \quad \text{at} \;\; z = \pm L/2, \tag{6}$$

where the perpendicular component of the magnetic field perturbation is defined as

$$\mathbf{b}_\perp = \mathbf{b} - \mathbf{e}_z b_z. \tag{7}$$

Since the tube boundary consists of magnetic field lines which are frozen in the dense plasma in the regions $|z| \geq L/2$, it follows that

$$\eta = 0 \quad \text{at} \quad z = \pm L/2. \tag{8}$$

It is straightforward to verify that this boundary condition is consistent with Equations (4)-(6).

The system of equations (2) and the boundary conditions (3)-(6) and (8) will be used in the next section to derive the governing equation for kink oscillations of a loop with non-stationary density and plasma flow.

3. Derivation of the governing equation

The system of equations (2) can be transform to

$$\frac{\partial \mathbf{v}}{\partial t} + U\frac{\partial \mathbf{v}}{\partial z} = -\frac{1}{\rho}\nabla_\perp P + \frac{B}{\mu_0 \rho}\frac{\partial \mathbf{b}_\perp}{\partial z}, \tag{9a}$$

$$\frac{\partial \mathbf{b}_\perp}{\partial t} + \frac{\partial (U\mathbf{b}_\perp)}{\partial z} = B\frac{\partial \mathbf{v}}{\partial z}, \tag{9b}$$

$$\frac{\partial P}{\partial z} = -\frac{B}{\mu_0}\nabla_\perp \cdot \mathbf{b}_\perp. \tag{9c}$$

Here the perpendicular gradient operator $\nabla_\perp$ is defined by

$$\nabla_\perp = \nabla - \mathbf{e}_z \frac{\partial}{\partial z}. \tag{10}$$

The characteristic spatial scale of variation of all variables in the z-direction is L, while it is a in the r-direction. Since the tube is thin, $a/L = \epsilon \ll 1$. To take this difference in scales into account explicitly we introduce the stretching variable $\sigma = \epsilon^{-1} r$. Then, eliminating $\mathbf{v}$ from Equations (9a) and (9b) we obtain

$$\left(\frac{\partial}{\partial t} + \frac{\partial}{\partial z}U\right)^2 \mathbf{b}_\perp - \frac{\partial}{\partial z}\left(V_A^2 \frac{\partial \mathbf{b}_\perp}{\partial z}\right) = -\epsilon^{-1}\frac{\partial}{\partial z}\left(\frac{B}{\rho}\widetilde{\nabla}_\perp P\right), \tag{11}$$

where the square of the Alfvén speed is defined by $V_A^2 = B^2/\mu_0\rho$,

$$\widetilde{\nabla}_\perp P = \epsilon \nabla_\perp P = \mathbf{e}_r \frac{\partial P}{\partial \sigma} + \mathbf{e}_\varphi \frac{1}{\sigma}\frac{\partial P}{\partial \varphi}, \tag{12}$$

and $\mathbf{e}_r$ and $\mathbf{e}_\varphi$ are the unit vectors in the r- and φ-direction. Equation (11), in particular, implies that $P \sim \epsilon(B/\mu_0)|\mathbf{b}_\perp|$. Then it follows that the ratio of the left-hand side of Equation (9c) to its right-hand

side is of the order of ϵ^2. This implies that we can neglect the left-hand side of Equation (9c) in comparison with its right-hand side, and reduces this equation to

$$\widetilde{\nabla}_\perp \cdot \mathbf{b}_\perp \equiv \frac{1}{\sigma}\left(\frac{\partial(\sigma b_r)}{\partial\sigma} + \frac{\partial b_\varphi}{\partial\varphi}\right) = 0. \tag{13}$$

Applying the operator $\widetilde{\nabla}_\perp\cdot$ to Equation (9b) and using Equation (13) we obtain

$$\frac{\partial}{\partial z}\widetilde{\nabla}_\perp \cdot \mathbf{v} = 0. \tag{14}$$

The boundary condition (6) is an identity with respect to σ and φ. This implies that we can apply $\widetilde{\nabla}_\perp\cdot$ to this boundary condition and use Equation (13) to obtain

$$\widetilde{\nabla}_\perp \cdot \mathbf{v} = 0, \quad \text{at} \;\; z = \pm L/2. \tag{15}$$

It follows from Equations (14) and (15) that

$$\widetilde{\nabla}_\perp \cdot \mathbf{v} = 0. \tag{16}$$

Now, applying the operator $\widetilde{\nabla}_\perp\cdot$ to Equation (9a) rewritten in terms of the new independent variable σ and using Equations (13) and (16) we obtain

$$\widetilde{\nabla}^2_\perp P \equiv \frac{1}{\sigma}\frac{\partial}{\partial\sigma}\sigma\frac{\partial P}{\partial\sigma} + \frac{1}{\sigma^2}\frac{\partial^2 P}{\partial\varphi^2} = 0. \tag{17}$$

In what follows we only consider the kink oscillations and take perturbations of all variables proportional to $\exp(i\varphi)$. We only needed the stretching variable σ to neglect the small terms in the equations and derive Equation (17). Once this is achieved, we again start to use the variable r. As a result Equation (17) reduces to

$$r\frac{\partial}{\partial r}r\frac{\partial P}{\partial r} - P = 0. \tag{18}$$

The solution to this equation regular in the tube, decaying far from the tube, and satisfying boundary condition (3) is

$$P = q(t,z)\begin{cases} r, & r < a, \\ a^2/r, & r > a, \end{cases} \tag{19}$$

where, at present, $q(t,z)$ is an arbitrary function.

Let us write the r-component of Equation (9a) at the tube boundary inside and outside the tube and use Equation (19). As a result we obtain

$$\frac{\partial v_{r\mathrm{i}}}{\partial t} + U_\mathrm{i}\frac{\partial v_{r\mathrm{i}}}{\partial z} = -\frac{q}{\rho_\mathrm{i}} + \frac{B}{\mu_0\rho_\mathrm{i}}\frac{\partial b_r}{\partial z}, \tag{20a}$$

$$\frac{\partial v_{re}}{\partial t} + U_i \frac{\partial v_{re}}{\partial z} = \frac{q}{\rho_e} + \frac{B}{\mu_0 \rho_e} \frac{\partial b_r}{\partial z}. \tag{20b}$$

We do not write the indices 'i' and 'e' at b_r because, in accordance with Equation (5), b_r is the same at both sides of the boundary. Now, multiplying Equation (20a) by ρ_i, Equation (20b) by ρ_e, adding the results, and using Equation (4) and Equation (5), we arrive at the equation for η,

$$\rho_i \left(\frac{\partial}{\partial t} + U_i \frac{\partial}{\partial z} \right)^2 \eta + \rho_e \left(\frac{\partial}{\partial t} + U_e \frac{\partial}{\partial z} \right)^2 \eta - \frac{2B^2}{\mu_0} \frac{\partial^2 \eta}{\partial z^2} = 0. \tag{21}$$

Function η has to satisfy the boundary condition (8).

Recall that we canceled out the dependence on φ by assuming that the perturbations of all variables are proportional to $\exp(i\varphi)$. This implies that $\eta(t, z)$ is a complex-valued function, *i.e.* $\eta = \eta_R + i\eta_I$. To obtain the real-valued function we have to take $\Re(\eta)$ instead of η, where $\Re$ indicates the real part of a quantity. Then we obtain

$$\eta = \eta_R \cos\varphi - \eta_I \sin\varphi. \tag{22}$$

Let us introduce the Lagrangian displacement $\boldsymbol{\xi}_0 + \boldsymbol{\xi}$, where $\boldsymbol{\xi}_0$ is the Lagrangian displacement in the unperturbed state. Since the unperturbed flow is in the z-direction, $\boldsymbol{\xi}_0$ is also in the z-direction. The quantity $\boldsymbol{\xi}$ is the perturbation of the Lagrangian displacement. In the Lagrangian description the initial position is used to label a plasma element.

We also can use another approach to the description of the plasma motion called the quasi-Lagrangian. In this approach a plasma element is labeled by the position where it would be if the flow had not been perturbed (see, *e.g.*, Goedbloed, Poedts, and Keppens, 2010). In this description $\boldsymbol{\xi}$ is called the plasma displacement. It is related to the velocity perturbation by (*e.g.* Goossens, Hollweg, and Sakurai, 1992)

$$\mathbf{v} = \frac{\partial \boldsymbol{\xi}}{\partial t} + (\mathbf{v} \cdot \nabla)\boldsymbol{\xi} - (\boldsymbol{\xi} \cdot \nabla)\mathbf{U}. \tag{23}$$

Since $v_z = 0$ and $\mathbf{U} = U\mathbf{e}_z$, it follows from this equation that $\xi_z = 0$. Then, taking into account that the magnetic field lines are frozen in the plasma, we obtain that the equation of an arbitrary magnetic field line is $\mathbf{r}(t, z) = \mathbf{r}_0 + \boldsymbol{\xi}(t, z) + z\mathbf{e}_z$, where $\mathbf{r}$ is the position vector and $\mathbf{r}_0$ is an arbitrary constant vector. The magnetic field is tangent to the magnetic field line which, in the linear approximation, implies that

$$b_r = B \frac{\partial \xi_r}{\partial z} \qquad b_\varphi = B \frac{\partial \xi_\varphi}{\partial z}. \tag{24}$$

It follows from Equations (11) and (19) that $\mathbf{b}_\perp$ is independent of r inside the tube. Then, comparing Equations (5) and (24), taking into account that

$$\xi_r = \xi_\varphi = \eta = 0 \quad \text{at} \quad z = \pm L/2, \tag{25}$$

and using Equation (22), we immediately obtain

$$\xi_r = \eta_\mathrm{R} \cos\varphi - \eta_\mathrm{I} \sin\varphi. \tag{26}$$

Using Equations (5), (13) and the fact that $\mathbf{b}_\perp$ is independent of r, we easily obtain the expression for b_φ in terms of η_R and η_I. Then, using Equations (24) and (25), we arrive at

$$\xi_\varphi = -\eta_\mathrm{R} \sin\varphi - \eta_\mathrm{I} \cos\varphi. \tag{27}$$

Let us introduce the auxiliary Cartesian coordinates $x = r\cos\varphi$ and $y = r\sin\varphi$. Then it follows from Equations (26) and (27) that

$$\xi_x = \eta_\mathrm{R}, \quad \xi_y = -\eta_\mathrm{I} \quad \text{for} \quad r < a. \tag{28}$$

We see that the displacements of all point of the tube cross-section are the same and given by the vector $\boldsymbol{\xi}$ with the Cartesian components defined by Equation (28). This is the generalization of the result previously obtained for kink oscillations of magnetic tubes without flow (see, *e.g.*, Ruderman and Erdélyi, 2009). In particular, $\boldsymbol{\xi}$ determines the displacement of the tube axis. Since both η_R and η_I satisfy Equation (21), it follows that $\boldsymbol{\xi}$ also satisfies Equation (21). Hence, Equation (21) can be considered as an equation describing the displacement of the tube axis.

4. Standing kink oscillations of magnetic tubes with homogeneous density and flow velocity

Let us use Equation (21) with the boundary condition (8) to study the eigenmodes of kink oscillations of magnetic tubes in the case when both $\rho_{\mathrm{i,e}}$ and $U_{\mathrm{i,e}}$ are constant. To study the eigenmodes we take $\eta \sim \exp(-i\omega t)$. Then Equation (21) reduces to

$$(C_k^2 - V_2^2)\frac{d^2\eta}{dz^2} + 2i\omega V_1 \frac{d\eta}{dz} + \omega^2 \eta = 0, \tag{29}$$

where

$$C_k^2 = \frac{2B^2}{\mu_0(\rho_\mathrm{i} + \rho_\mathrm{e})}, \quad V_1 = \frac{\rho_\mathrm{i} U_\mathrm{i} + \rho_\mathrm{e} U_\mathrm{e}}{\rho_\mathrm{i} + \rho_\mathrm{e}}, \quad V_2^2 = \frac{\rho_\mathrm{i} U_\mathrm{i}^2 + \rho_\mathrm{e} U_\mathrm{e}^2}{\rho_\mathrm{i} + \rho_\mathrm{e}}. \tag{30}$$

Recall that C_k is the phase speed of kink oscillations of thin homogeneous magnetic tube without flow. The general solution to Equation (29) is

$$\eta = A_+ e^{ik_+ z} + A_- e^{ik_- z}, \tag{31}$$

where

$$k_\pm = \omega \frac{-V_1 \pm \sqrt{C_k^2 - V_3^2}}{C_k^2 - V_2^2}, \quad V_3^2 = V_2^2 - V_1^2 = \frac{\rho_\mathrm{i}\rho_\mathrm{e}(U_\mathrm{i} - U_\mathrm{e})^2}{(\rho_\mathrm{i} + \rho_\mathrm{e})^2}. \tag{32}$$

Substituting Equation (31) in the boundary condition (8) we obtain the system of two linear homogeneous algebraic equations for A_+ and A_-. This system has a non-trivial solution only when its determinant is zero. This condition gives the dispersion equation determining ω,

$$\exp\left(\frac{2i\omega L\sqrt{C_k^2 - V_3^2}}{C_k^2 - V_2^2}\right) = 1. \tag{33}$$

The non-negative solutions to this dispersion equation are

$$\omega_n = \frac{\pi n |C_k^2 - V_2^2|}{L\sqrt{C_k^2 - V_3^2}}, \quad n = 1, 2, \ldots \tag{34}$$

Here $n = 1$ corresponds to the fundamental harmonic, and $n > 1$ to the overtones. Since $V_3 < V_2$ it follows that $\omega_n < \pi C_k/L$ when the flow speed is moderate, *i.e.* when $C_k > V_2$. This result is not surprising at all. The period of the fundamental harmonic of a standing wave is equal to the time needed for a signal to travel from one end of the tube to the other and back. The travelling time in the direction of the flow is smaller than that in the absence of flow, and the travelling time in the opposite direction is larger than that in the absence of flow. It is well known that the sum of the two times is larger than the twice the travelling time in the absence of flow.

The frequency becomes imaginary, which means instability, when $C_k^2 < V_3^2$. When $C_k^2 - V_3^2 \to 0$, $\omega_n \to \infty$, which is unphysical. However, when deriving Equation (21), we assumed that the characteristic time is of the order of Alfvénic time along the loop, which is of the order of L/C_k. Hence, Equation (21) and, consequently, Equation (29) does not describe oscillations with a frequency much larger than $\pi C_k/L$.

It is also instructive to give the expressions for the eigenfunctions:

$$\eta_n = \exp\left(\frac{i\pi n V_1 \mathrm{sign}(V_2^2 - C_k^2)}{L\sqrt{C_k^2 - V_3^2}} z\right) \begin{cases} \cos\dfrac{\pi n z}{L}, & n \text{ odd}, \\ \sin\dfrac{\pi n z}{L}, & n \text{ even}. \end{cases} \tag{35}$$

We see that the eigenfunctions are complex, and they are neither even nor odd. Once again it is an expected result because the flow destroys the symmetry with respect to the z-direction.

5. Eigenvalue problem: general analysis

In this section we study the general properties of the eigenvalue problem for Equation (21). As in the previous section we take $\eta \sim \exp(-i\omega t)$. The plasma densities and flow velocities are related by the mass conservation equation,

$$\rho_{\rm i} U_{\rm i} = \text{const}, \qquad \rho_{\rm e} U_{\rm e} = \text{const}, \tag{36}$$

otherwise $\rho_{\rm i,e}$ and $U_{\rm i,e}$ are arbitrary functions of z. Now Equation (21) reduces to

$$C_k^2 \frac{d^2\eta}{dz^2} - \frac{1}{\rho_{\rm i}+\rho_{\rm e}} \frac{d}{dz}(\rho_{\rm i}+\rho_{\rm e}) V_2^2 \frac{d\eta}{dz} + 2i\omega V_1 \frac{d\eta}{dz} + \omega^2 \eta = 0, \tag{37}$$

where C_k, V_1 and V_2 are still defined by Equation (30), but now they are functions of z. Observations show that the flow velocities in the corona do not exceed about 100 km/s, while C_k is at least a few hundred km/s. Hence, in what follows we assume that $V_2(z) < C_k(z)$ for $z \in [-L/2, L/2]$.

Let us introduce new variables

$$u = \int_{-L/2}^{z} \frac{\psi_{\rm f}\, dz'}{\psi(z')}, \quad q = \eta \exp(i\alpha\omega u), \tag{38}$$

where

$$\psi(z) = (\rho_{\rm i}+\rho_{\rm e})(C_k^2 - V_2^2), \quad \alpha = \frac{\rho_{\rm i} U_{\rm i} + \rho_{\rm e} U_{\rm e}}{\psi_{\rm f}}, \quad \psi_{\rm f} = \psi(-L/2). \tag{39}$$

It follows from Equation (29) that $\alpha = \text{const}$. Since $u(z)$ is a monotonically increasing function, there is the inverse function $z(u)$ which is also monotonically increasing. In the new variables, Equations (37) and (8) reduce to

$$\frac{d^2 q}{du^2} + \omega^2 W(u) q = 0, \tag{40}$$

$$q = 0 \quad \text{at} \quad u = 0,\, u_0, \tag{41}$$

where

$$W(u) = \frac{1}{\psi_{\rm f}^2}\{(\rho_{\rm i}+\rho_{\rm e})^2 C_k^2 - \rho_{\rm i}\rho_{\rm e}(U_{\rm i}-U_{\rm e})^2\}, \quad u_0 = \int_{-L/2}^{L/2} \frac{\psi_{\rm f}\, dz}{\psi(z)}. \tag{42}$$

Equations (40) and (41) constitute the classical Sturm-Liouville problem for a second-order differential equation with ω^2 the eigenvalue. In accordance with the theory of Sturm-Liouville problem the eigenvalues are real and constitute a monotonically increasing unbounded sequence (see *e.g.* Coddington and Levinson, 1955). The first eigenvalue is the square of the fundamental frequency, and the corresponding eigenfunction has no nodes in $(0, u_0)$. All other eigenmodes are the squares of frequencies of overtones. The eigenfunction corresponding to the nth overtone has $n-1$ nodes in $(0, u_0)$.

Since $W(u)$ is real, we can always take q to be real. Multiplying Equation (40) by q, integrating from 0 to u_0, and using Equation (41) we obtain

$$\omega^2 \int_0^{u_0} W(u) q^2 \, du = \int_0^{u_0} \left(\frac{dq}{du}\right)^2 du. \tag{43}$$

Since $\rho_{\rm i}\rho_{\rm e}(U_{\rm i} - U_{\rm e})^2 < (\rho_{\rm i} + \rho_{\rm e})^2 V_2^2$, it follows from the assumption $V_2 < C_k$ that $W(u) > 0$. Then Equation (43) implies that $\omega^2 > 0$, *i.e.* all eigenvalues of the Sturm-Liouville problem (40), (41) are positive.

6. Eigenmodes of kink oscillations of coronal loops with siphon flows

In this section we study the effect of siphon flows on kink oscillations of coronal loops. We start our analysis describing the equilibrium state.

6.1. Equilibrium state

Siphon flows in coronal loops have been extensively studied (see *e.g.* Orlando, Peres, and Serio, 1995, and references therein). In particular, siphon flows caused by the pressure difference at two coronal loop foot points and by asymmetric heat deposition have been investigated (*e.g.* Betta *et al.*, 1999). However, we do not want to embark on a long discussion of different complicated mechanisms that can be responsible for the appearance of siphon flows because the aim of our analysis is not to study siphon flows themselves but only to investigate their effect on coronal loop kink oscillations. In accordance with this, we adopt a very simple model of siphon flow where the flow is "caused" by the boundary condition at one of the loop foot points. We simply assume that the flow velocity is fixed and equal to $U_{\rm f} > 0$ at this foot point.

We consider a loop that has a half-circle shape with the constant circular cross-section of radius a. The atmosphere is isothermal and the temperatures inside and outside the loop are the same. The plasma

outside the loop is at rest, so that $U_e = 0$. Then we immediately obtain that the density outside the loop is given by

$$\rho_e(z) = \frac{\rho_\mathrm{f}}{\zeta} \exp\left(-\frac{L}{\pi H}\cos\frac{\pi z}{L}\right), \tag{44}$$

where H is the atmospheric scale height, ρ_f the density inside the loop at the foot points, and $\zeta > 1$ the ratio of densities inside and outside the loop at the foot points. Inside the loop there is a flow with the velocity $U_\mathrm{i} = U$. The plasma density and velocity inside the loop are related by the mass conservation law,

$$\rho_\mathrm{i}(z)U(z) = \rho_\mathrm{f}U_\mathrm{f}, \tag{45}$$

The density and flow speed inside the tube has also to satisfy the momentum equation. For an isothermal motion this equation takes the form

$$U\frac{dU}{dz} = -g\left(\frac{H}{\rho_\mathrm{i}}\frac{d\rho_\mathrm{i}}{dz} - \sin\frac{\pi z}{L}\right), \tag{46}$$

where g is the gravity acceleration and the last term of the right-hand side of this equation represents the projection of the gravity acceleration on the tangent to the loop axis. Integrating this equation we obtain

$$\frac{U^2}{2} + gH\ln\frac{\rho_\mathrm{i}}{\rho_\mathrm{f}} = \frac{U_\mathrm{f}^2}{2} - \frac{gL}{\pi}\cos\frac{\pi z}{L}, \tag{47}$$

Using Equation (45) we can reduce this equation to

$$f(\kappa) \equiv \chi\left(\frac{1}{\kappa^2} - 1\right) + 2\ln\kappa = -\frac{2L}{\pi H}\cos\frac{\pi z}{L}, \tag{48}$$

where

$$\chi = \frac{U_\mathrm{f}^2}{gH}, \qquad \kappa = \frac{\rho_\mathrm{i}}{\rho_\mathrm{f}}. \tag{49}$$

The solution describing the flow in the loop exists only when there is a solution to Equation (48) defining κ as a single-valued function of z for $z \in [-L/2, L/2]$. Function $f(\kappa)$ takes its minimum equal to $f_m(\chi) = 1-\chi+\ln\chi$ at $\kappa = \sqrt{\chi}$. Function $f(\kappa)$ monotonically decreases from ∞ to $f_m(\chi)$ on the interval $(0, \sqrt{\chi})$, and monotonically increases from $f_m(\chi)$ to ∞ on the interval $(\sqrt{\chi}, \infty)$. It is straightforward to see that Equation (48) has solutions for any $z \in [-L/2, L/2]$ if and only if

$$\frac{L}{\pi H} \le \frac{L_M}{\pi H} = -\frac{f_m(\chi)}{2} \equiv \frac{1}{2}(\chi - 1 - \ln\chi). \tag{50}$$

Figure 1 shows the graph of $f(\kappa)$ and illustrates the analysis. The dependence of the maximum possible ratio of the coronal loop height to the atmospheric scale height, $L_M/\pi H$, on χ is shown in Figure 2.

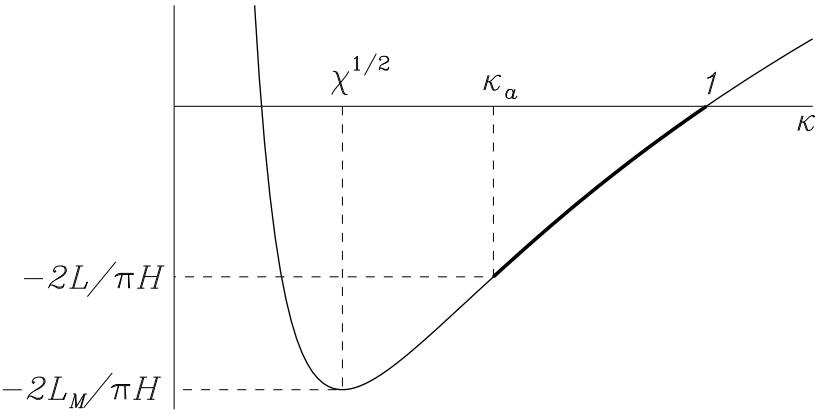

Figure 1. The graph of function $f(\kappa)$. The bold curve shows the part of this graph corresponding to the solution of Equation (48) describing the dependence of κ on z in the coronal loop.

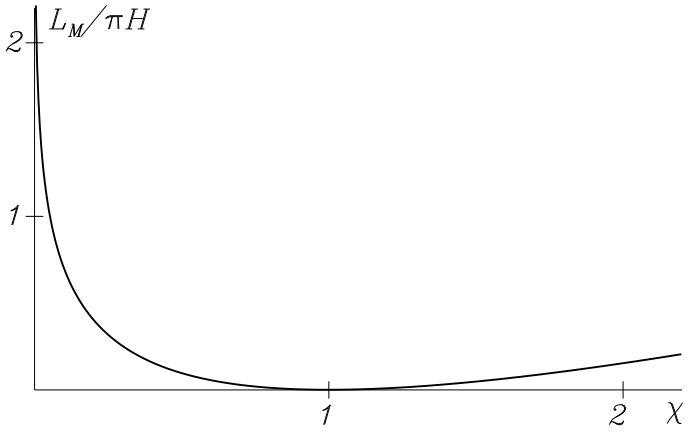

Figure 2. The dependence of the maximum possible ratio of the coronal loop height to the atmospheric scale height, $L_M/\pi H$, on χ.

It follows from the analysis and is also obvious by inspection of Figure 1 that, when $L \leq L_M$, there are two solutions of Equation (48) for any $z \in [-L/2, L/2]$. These solutions define two continuous functions on the interval $[-L/2, L/2]$, $\kappa_1(z)$ and $\kappa_2(z)$. These functions satisfy the inequalities $\kappa_1(z) \leq \sqrt{\chi}$ and $\kappa_2(z) \geq \sqrt{\chi}$. In the solar atmosphere $g \approx 274\,\mathrm{m/s^2}$. As we have already mentioned, the observed flow velocities do not exceed 100 km/s, so that we can take $U_\mathrm{f} \lesssim 100$ km/s. Then, taking $H \sim 60\,\mathrm{Mm}$, we obtain $\chi \lesssim 0.61 < 1$. Since $\kappa(-L/2) = 1$,

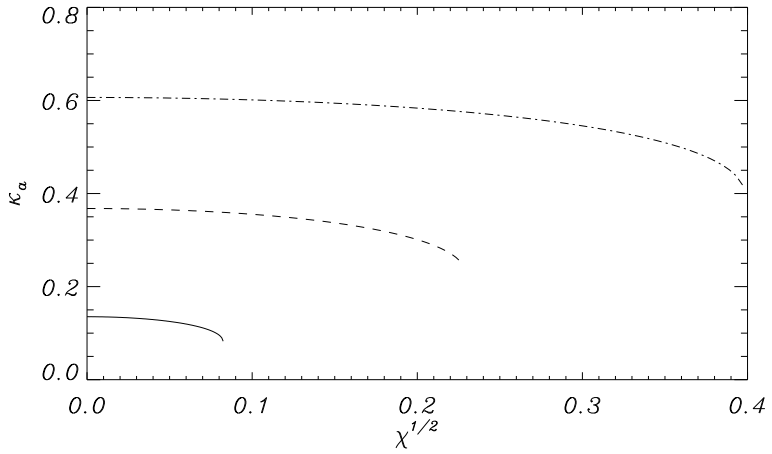

Figure 3. The dependence of κ_a on χ. The dash-dotted, dashed and solid curves correspond to $L/\pi H = 0.5$, 1 and 2 respectively. Each curve shows he dependence of κ_a on χ for $0 \le \chi \le \chi_M$.

this result implies that we have to choose the solution $\kappa_2(z)$. In what follows we will drop the subscript '2'.

If we fix $L/\pi H$ then it follows from the previous analysis that, under the assumption that $\chi < 1$, there is a maximum value of χ, $\chi_M(L/\pi H)$, such that the equilibrium exists only for $\chi \le \chi_M$. The dependence of χ_M on $L/\pi H$ is shown in Figure 2. To find χ_M corresponding to a given $L/\pi H$ we need to find the point on the graph shown in Figure 2 with the ordinate equal to $L/\pi H$. The abscissa of this point gives χ_M. In particular, $\chi_M \approx 0.16$, 0.052 and 0.0068 for $L/\pi H = 0.5$, 1 and 2 respectively. For $H = 60\,\mathrm{Mm}$ these values correspond to $U_\mathrm{f} \approx 51$ km/s, 29 km/s and 10.5 km/s respectively.

We can consider κ as a function of two variables: the length along the loop z and the parameter χ. Then, differentiating Equation (48) with respect to χ we obtain

$$\frac{\partial \kappa}{\partial \chi} = \frac{\kappa(1-\kappa^2)}{2(\chi-\kappa^2)}. \tag{51}$$

Since $\sqrt{\chi} < \kappa \le 1$, it follows from this equation that, at any fixed z, κ is a monotonically decreasing function of χ, *i.e.* the density in the loop decreases when U_f increases. In particular, the density at the loop apex, $\rho_\mathrm{f}\kappa_a$, is a decreasing function of χ. In Figure 3 the dependence of κ_a on $\sqrt{\chi}$ is shown for $L/\pi H = 0.5$, 1 and 2. We can see that the presence of the flow practically does not affect κ_a unless the flow velocity is close

to its maximum value. In fact, this is true not only for the apex point, but for the whole loop.

Finally, we point out one interesting property of the model presented in this section. It turns out that, when U_f takes its maximum possible value, U_{fM}, the velocity at the apex point is independent of the loop length L. Let us prove this. In accordance with Equation (48), when $\chi = \chi_M$, we have the relation

$$\chi_M \left(\frac{1}{\kappa_a^2} - 1 \right) + 2 \ln \kappa_a = -\frac{2L}{\pi H}. \tag{52}$$

On the other hand χ_M is related to the loop length by

$$\chi_M - 1 + \ln \chi_M = \frac{2L}{\pi H}. \tag{53}$$

Substituting Equation (52) in Equation (53) we obtain

$$\frac{\chi_M}{\kappa_a^2} + \ln \frac{\chi_M}{\kappa_a^2} = 1, \tag{54}$$

which implies that $\chi_M/\kappa_a^2 = 1$. This equality can be rewritten as $U_{fM}^2 \rho_\mathrm{f}^2 = \rho_{\mathrm{i}a}^2 gH$, where $\rho_{\mathrm{i}a}$ is the density inside the tube at the apex point. Then, using Equation (45), we obtain for the velocity at the apex point $U_a = \sqrt{gH}$. For $H = 60\,\mathrm{Mm}$ we have $U_a \approx 128$ km/s.

6.2. The effect of flow on the eigenmode frequencies

In this subsection we study the effect of flow on the frequencies of eigenmodes of kink oscillations using the model described in the previous subsection. To determine the eigenfrequencies we numerically solved Equation (40) with the boundary conditions (41). In dimensionless variables the dimensionless frequency $\Omega = \omega/\omega_\mathrm{f}$ depends on three dimensionless parameter, χ, $L/\pi H$ and gH/C_f^2, where $\omega_\mathrm{f} = \pi C_\mathrm{f}/L$ is the fundamental harmonic frequency of a homogeneous loop that we obtain if we take $H \to \infty$. If we take $H = 60$ Mm, then, for realistic values of C_f, *i.e.*, for $C_\mathrm{f} \gtrsim 600$ km/s, we obtain that $gH/C_\mathrm{f}^2 \lesssim 0.05$. In Figure 4 the dependence of $\Omega = \omega/\omega_\mathrm{f}$ on χ is shown for the fundamental harmonic for different values of $L/\pi H$ and gH/C_f^2.

We also calculated the dependence of the ratio of frequencies of the first overtone and fundamental harmonic, R, on χ for different values of $L/\pi H$ and gH/C_f^2. This dependence is shown in Figure 5. We can see that both the fundamental harmonic frequency and the ratio of frequencies of the first overtone and fundamental harmonic are practically independent of the parameter gH/C_f^2. This is, of course, not surprising at all because gH/C_f^2 is of the order of plasma β which

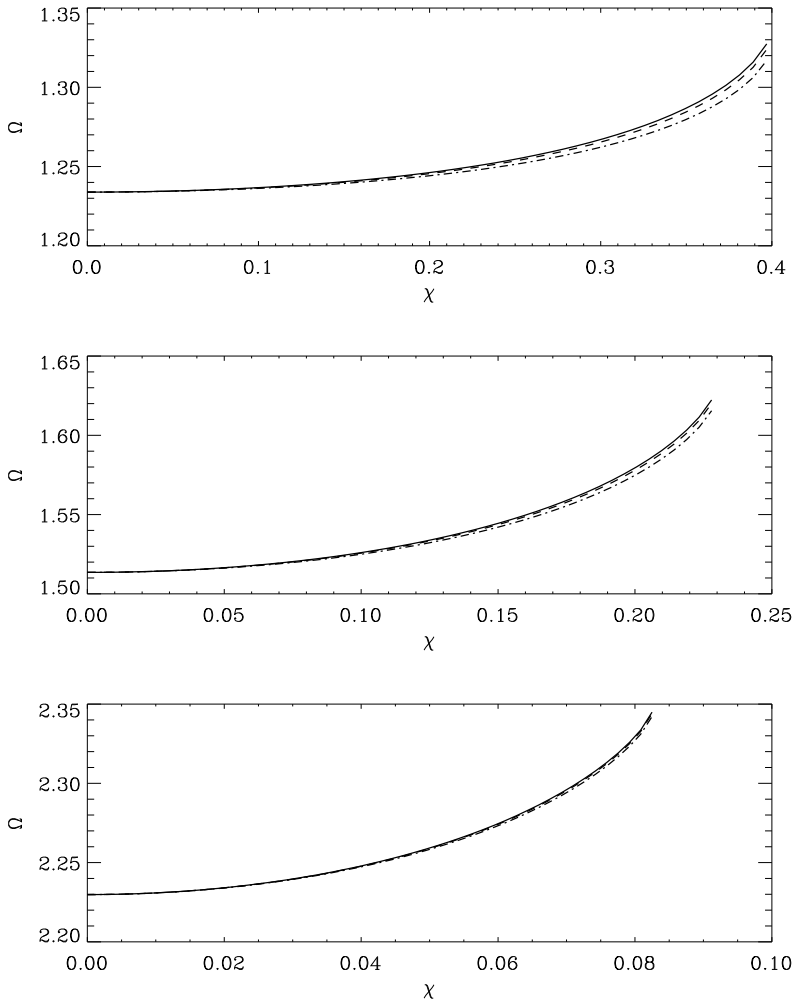

Figure 4. The dependence of the dimensionless fundamental frequency Ω on χ for $\chi \in [0, \chi_M]$. The upper, middle and lower panel correspond to $L/\pi H = 0.5$, 1 and 2 respectively. The solid, dashed and dash-dotted curves correspond to $gH/C_{\rm f}^2 = 0.02$, 0.03 and 0.05 respectively. For $H = 60$ Mm these values of $gH/C_{\rm f}^2$ correspond to $C_{\rm f} \approx 905$, 739 and 572 km/s respectively.

is very small in the solar corona. We can also see that both the fundamental frequency and the frequency ratio only slightly depend on the parameter χ characterizing the intensity of the siphon flow. Still Figure 4 shows that the fundamental frequency is an increasing function of χ. In Section 4 we showed that the presence of flows decreases the oscillation frequency and gave a simple physical explanation of this effect. Does the result obtained in this section contradict that obtained

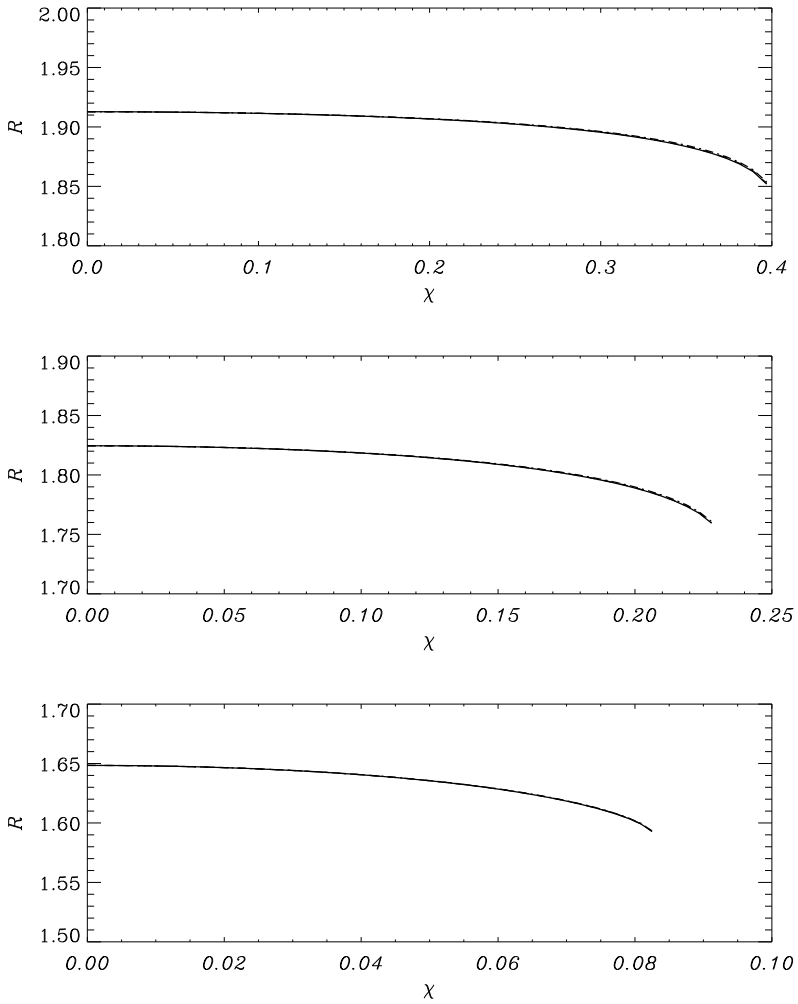

Figure 5. The dependence of the ratio of frequencies of the first overtone and fundamental harmonic, R, on χ for $\chi \in [0, \chi_M]$. The upper, middle and lower panel correspond to $L/\pi H = 0.5$, 1 and 2 respectively. The solid, dashed and dash-dotted curves correspond to $gH/C_{\rm f}^2 = 0.02$, 0.03 and 0.05 respectively, however these curves are practically indistinguishable.

in Section 4? It does not at all. The presence of the flow still tends to increase the signal travelling time and thus to decrease the oscillation frequency. However, as it follows from Figure 3, at the same time the presence of the flow results in the decrease of the plasma density in the tube which, in turn, leads to the increase of the oscillation frequency. Figure 4 simply shows that the second effect dominates the first one.

The results that siphon flows only slightly affect both the fundamental frequency and the ratio of frequencies of the first overtone and fundamental harmonic should be considered as good news for coronal seismology. Nakariakov and Ofman (2001) were the first who used the observations of coronal loop kink oscillations to estimate the magnetic field magnitude in the corona. After Verwichte *et al.* (2004) reported first simultaneous observations of the fundamental harmonic and first overtone of coronal look kink oscillations Andries, Arregui, and Goossens (2005) suggested to use these observations to estimate the atmospheric scale height H in the corona.

In the first coronal seismology studies based on observations of coronal loop kink oscillations very simple models of coronal loops were used. Nakariakov and Ofman (2001) modelled the coronal loop as a straight homogeneous magnetic tube. Andries, Arregui, and Goossens (2005) assumed that a loop has a half-circle shape and constant circular cross-section, and the plasma temperature inside and outside the loop is constant. The question arises as to how robust the seismological results are? Will they change sufficiently if we use more realistic and sophisticated models of coronal loops? Ruderman, Verth, and Erdélyi (2008) and Verth, Erdélyi, and Jess (2008) have shown that the account of the loop expansion can strongly affect the estimates of the coronal scale height. Dymova and Ruderman (2006) and Morton and Erdélyi (2009) have found that the account of the loop shape can moderately affect this quantity. Finally, Ruderman (2007) has shown that the twist of magnetic field lines in the loop can be safely neglected when estimating the atmospheric scale height in the corona. Now we can extend the list of unimportant parameters. It follows from the results presented in this section that the presence of siphon flows in coronal loops can hardly affect the seismological results obtained on the basis of observations of coronal loop kink oscillations.

7. Summary and conclusions

In this paper we have studied non-axisymmetric oscillations of a thin magnetic tube with the time-dependent density and plasma flow. Using the thin tube approximation we derived the general governing equation for kink oscillations in the thin tube approximation. Then we used this equation to study the effect of stationary steady flow on the coronal loop kink oscillations. We have used a simple model of siphon flow where the flow is "caused" by the boundary condition at one foot point and assumed that the flow velocity at this foot point is fixed. Then we numerically studied the flow effect on the frequency of the fundamental

harmonic of kink oscillations, and on the ratio of frequencies of the first overtone and fundamental harmonic.

The main results can be summarized as follows. For all flow velocities admissible in the stationary state used in our analysis the effect of flow on both the fundamental harmonic of kink oscillations and on the ratio of frequencies of the first overtone and fundamental harmonic is very weak. An important conclusion that we have made on the basis of these results is that to take into account stationary siphon flows is unimportant for the estimates of the atmospheric scale height obtained on the basis of observations of the coronal loop kink oscillations. However, we should emphasize that these results are obtained under the assumption that the equilibrium state is stationary, so that neigher the plasma density nor velocity change with time. The results could be quite different for time-dependent equilibrium states as has been shown by Morton and Erdélyi (2009).

Acknowledgements

The author acknowledges the support by the STFC grant.

References

Andries, J., Arregui, I., Goossens, M.: 2005, *Astrophys. J.* **624**, L57.
Betta, R., Orlando, S., Peres, G., Serio, S.: 1999, *Sol. Phys.* **175**, 511.
Brekke, P., Kjeldseth-Moe, O., Harrison, R. A.: 1997, *Space Sci. Rev.* **87**, 133.
Coddington, E. A., Levinson, N.: 1955, *Theory of Ordinary Differential Equations.* McGraw-Hill: New-York.
Chae, J., Ahn, K., Lim, E.-K., Choe, G. S., Sakurai, T.: 2008, *Astrophys. J.* **689**, L73.
Dymova, M., Ruderman, M. S.: 2006, *Astron. Astrophys.* **459**, 241.
Goedbloed, J. P., Poedts, S.. Keppens, R.: 2010, *Advanced Magnetohydrodynamics* Cambridge Univ. Press: Cambridge.
Goossens, M., Hollweg, J. V., Sakurai, T.: 1992, *Sol. Phys.* **138**, 233.
Gruszecki, M., Murawski, K., Ofman, L.: 2008, *Astron. Astrophys.* **488**, 757. Gruszecki2008
Morton, R. J., Erdélyi, R.: 2009, *Astron. Astrophys.* **502**, 315.
Nakariakov, V., Ofman, L.: 2001, *Astron. Astrophys.* **372**, L53.
Ofman, L., Wang, T. J.: 2008, *Astron. Astrophys.* **482**, L9.
Orlando, S., Peres, G., Serio, S.: 1995, *Astron. Astrophys.* **294**, 867.
Ruderman, M. S.: 2007, *Sol. Phys.* **246**, 119.
Ruderman, M. S., Erdélyi, R.: 2009, *Space Sci. Rev.* **149**, 199.
Ruderman, M. S., Verth, G., Erdélyi, R.: 2008, *Astrophys. J.* **686**, 694.
Terradas, J., Arregui, I., Oliver, R., Ballester, J. L.: 2008, *Astrophys. J.* **678**, L153.
Terradas, J., Goossens, M., Ballai, I.: 2010, *Astron. Astrophys* **515**, A46.
Verth, G., Erdélyi, R., Jess D. B.: 2008, *Astrophys. J.* **687**, L45.

Verwichte, E., Nakariakov, V., Ofman, L., DeLuca, E. E.: 2004, *Sol. Phys.* **223**, 77.
Winebarger, A. R., DeLuca, E. E., Golub, L.: 2001, *Astrophys. J.* **553**, L81.
Winebarger, A. R., Warren, H., van Ballegooijen, A., DeLuca, E. E., Golub, L.: 2002, *Astrophys. J.* **567**, L89.